(12)

LEVEL II

NRL Memorandum Report 4530

ADA099809

Dark-Field Study of Rear-Side Density Structure in Laser-Accelerated Foils

J. A. Stamper, S. H. Gold, S. P. Obenschain, E. A. McLean

Laser Plasma Branch
Plasma Physics Division

L. Sica

Applied Optics Branch
Optical Sciences Division

June 8, 1981

NAVAL RESEARCH LABORATORY
Washington, D.C.

(14) NRL-MR-4530

SECURITY CLASSIFICATION OF THIS PAGE (When Data Entered)

REPORT DOCUMENTATION PAGE

READ INSTRUCTIONS BEFORE COMPLETING FORM

1. REPORT NUMBER: NRL Memorandum Report 4530	2. GOVT ACCESSION NO.: AD-A099809	3. RECIPIENT'S CATALOG NUMBER
4. TITLE (and Subtitle): DARK-FIELD STUDY OF REAR-SIDE DENSITY STRUCTURE IN LASER-ACCELERATED FOILS		5. TYPE OF REPORT & PERIOD COVERED: Interim report on a ~~continuing~~ NRL problem.
		6. PERFORMING ORG. REPORT NUMBER
7. AUTHOR(s): J. A. Stamper, S. H. Gold, S. P. Obenschain, E. A. McLean, ~~and~~ L. Sica		8. CONTRACT OR GRANT NUMBER(s)
9. PERFORMING ORGANIZATION NAME AND ADDRESS: Naval Research Laboratory, Washington, DC 20375		10. PROGRAM ELEMENT, PROJECT, TASK AREA & WORK UNIT NUMBERS: 47-0859-0-1
11. CONTROLLING OFFICE NAME AND ADDRESS: U. S. Department of Energy, Washington, DC 20545		12. REPORT DATE: June 1981
		13. NUMBER OF PAGES: 20
14. MONITORING AGENCY NAME & ADDRESS (if different from Controlling Office)		15. SECURITY CLASS. (of this report): UNCLASSIFIED
		15a. DECLASSIFICATION/DOWNGRADING SCHEDULE

16. DISTRIBUTION STATEMENT (of this Report)

Approved for public release; distribution unlimited.

17. DISTRIBUTION STATEMENT (of the abstract entered in Block 20, if different from Report)

18. SUPPLEMENTARY NOTES

19. KEY WORDS (Continue on reverse side if necessary and identify by block number)

Laser fusion
Ablative acceleration
Laser probing
Dark field

20. ABSTRACT (Continue on reverse side if necessary and identify by block number)

A dark-field, laser-probing diagnostic has produced the first high-resolution photographs of density structure on the rear side of laser-accelerated foils. This diagnostic allows the preferential sampling of the steep-gradient region of an expanding plasma and permits two-dimensional, multiple-time recordings on a single photograph. The studies are aimed at understanding the early-time physics of target implosions for intertial-confinement fusion. Both long (500 psec) and short (150 psec) probe pulses were used to

(Continues)

DD FORM 1473, 1 JAN 73 EDITION OF 1 NOV 65 IS OBSOLETE
S/N 0102-014-6601

SECURITY CLASSIFICATION OF THIS PAGE (When Data Entered)

20. ABSTRACT (Continued)

study the rear-side plasmas of thin foils accelerated by the rocket-like reaction to a hot plasma ablated from the front side by the laser radiation. The longer pulse results, both for angular scatter and the life-time of small, transverse structure, imply a relatively cold (1 eV) rear side plasma. The short pulses provide high resolution photographs of the complete structure. One of these was a vortex-like structure, suggestive of the remnants of a hydrodynamic instability. These observations are relevant to two of the basic requirements of inertial-confinement fusion: cold fuel isentrope and implosion symmetry.

DARK-FIELD STUDY OF REAR-SIDE DENSITY STRUCTURE IN LASER-ACCELERATED FOILS

The ablative acceleration of thin foil targets is being studied[1] as a means of understanding the early-time physics of target implosions for inertial confinement fusion.[2] A dark-field, laser-probing diagnostic has produced the first, high-resolution (5 micron) photographs of density structure on the rear side (away from laser) of the foil targets. The study supports the earlier spectroscopic measurement[3] of a relatively cold ($\lesssim$10 eV) rear-side plasma and shows density modulations. These observations are relevant to two of the basic requirements or "critical elements" of high-gain, inertial confinement fusion:[4] that the fuel remain cold (isentropic compression) and that the implosion be symmetric.

This dark-field diagnostic has the advantage of preferentially sampling the steep gradient region of an expanding plasma and permitting two-dimensional, multiple-time recordings on a single photograph. Fine-scale (5-10 micron) structure, transverse to the direction of motion, was first seen with longer pulse (500 psec) probing and the complete structure was then resolved with shorter (150 psec) pulse probing. A striking vortex-like structure, with dimensions around 30 microns, was seen on one shot. This is suggestive of the remnants of a hydrodynamic instability. Smaller-scale structure, superimposed on a generally uniform acceleration, was seen on other shots.

The experimental arrangement is shown in Fig. 1. The NRL Pharos II main laser beam (100-500J in 4 nsec at 1.054 micron) is focused to a 1 mm diameter spot on the front side of a thin foil target (4-15 micron of CH plastic or Al). The irradiance is in the range .2 to 1 x 10^{13} W/cm^2. A probing laser beam is incident from the right, parallel to the target

Manuscript submitted April 9, 1981.

surface. Two types of probe pulses were used: (1) a (green) second harmonic pulse (5270 Å) chopped by a Pockels cell to a 500-psec width, and (2) a (red) pulse (6258 Å) produced by focusing the chopped green pulse into an ethanol cell and utilizing the backward Raman scattering.[5] This Raman pulse consisted of 2 to 3 sub-pulses having a width of 30 psec and spaced 80 psec apart to give an envelope of about 150 psec. Four pulses were produced (by beam-splitting) for some of the green-light probing but, for most of the data discussed here, only a single red pulse (envelope) was used.

The target is placed at the front focus of lens L_1 (f/2, 10 cm) and a second lens L_2 (f/10, 50 cm) is placed at the sum of the focal lengths (60 cm) from the first. The f/2 collection optics allows the collection of scattered light out to ± 14 degrees from the axis. The film is located at the back focal plane of the second lens. An opaque mask is placed either just in front of L_1 (position A) or at its back-focal-plane (position B). The mask had a diameter of 5 mm and was at position B for most of the data. Probe light that is not deflected by the target plasma is focused by L_1 and blocked by the mask to produce a dark background. However, probe light that passes through the leading (steep gradient) region of the rear-side plasma is deflected and then collimated by L_1 to get past the mask. Thus, a bright profile of this region is recorded on the dark background. If several pulses are used and spaced in time so that the velocity is sufficient to avoid image superposition, then several bright profiles are recorded on a single dark-field background photograph.[6] Because of the larger dynamic range and better spatial resolution on the negative (Polaroid type 55), we have primarily used the data as recorded on the negatives. We show here negative prints. Thus, the dark background is seen in the figures as a light background and the bright profiles are seen as dark bands.

The basic (assuming a planar object) performance of the optical system can be analyzed with standard Fourier transform methods.[7] From the diameter of the target region, the diameters (5 cm) and spacings of the lenses, and an observed half-angle limit of 8 degrees for the scattered light, one can conclude that the scattered probe light is fully collected by both lenses. Thus, the recorded intensity for a bright-field (no mask) illumination would depend only on amplitude variations in the object plane. However, for dark field imaging, the recorded intensity would depend on both amplitude and phase. This technique is analogous to the Schlieren and central dark ground methods[8] but utilizes a rather large mask to accentuate the steep-gradient, high-density region. Calculating the coherent transfer function of the system[7] shows that the light field U in the film plane can be expressed as $A(x) \exp\left[i\, \phi (x) \right] - C$, where A, a real positive function, and C a complex function, depend on the light field in the object plane. The function C is due to the mask at B. In the limit of a very small mask, C is a constant (the average of the field over the aperture) and, for the actual mask used (which blocks a 3° half-angle), it varies somewhat slowly compared to A and ϕ. Both A and ϕ are constant if there is no plasma. Thus, for a dark field image, the recorded intensity UU^* would depend on both the amplitude and phase variations caused by the plasma. If the mask at B is removed, then C vanishes so that the recorded bright-field intensity would depend only on the amplitude of the field at the target.

We now consider, qualitatively, the performance of the optical system in the actual experiment. There are contributions from throughout the active (plasma) region of finite extent about the object plane. Both bright-field and dark-field shadowgrams were taken (shown in Fig. 2) with the longer pulses. These showed similar fine-scale structure transverse to the direction of motion. There is evidence that scattering (refraction and diffraction) and absorption are both contributing to the recorded data. Diffraction lengths for the small-scale (5-20 microns) structure was comparable to the depth of the active region so that amplitude variations at one location are related to phase variations at another location. The 3-degree deflection required for the dark-field data depends on transverse phase variations. Further information (discussed later) indicates that absorption is also important and may dominate the bright field data. One type of plasma structure that is consistent with both results is a distribution of small, relatively cold (absorbing) plasma blobs with diffuse exteriors. Diffraction and refraction in the less dense exteriors can account for the dark-field data while the absorption of rays directed into the interiors can account for the bright-field data.

Before proceeding with a discussion of experimental results, a brief background discussion is given of physical processes affecting the observed rear-side plasma: Due to laser irradiation, a rather hot (few hundred eV) plasma is ablated from the front (laser) side of the foil target. The target is accelerated by the rocket-like reaction to this blow-off plasma. A small fraction of the incident laser energy is transported through the interior of the accelerating target by a variety of mechanisms, including thermal conduction, shocks and x-ray preheat. The early-time expansion of the relatively cold, rear-side plasma is inhibited by the acceleration. Most of the data presented here was taken 2.5 nsec after the peak of the main laser pulse, when the acceleration was small. The data shows a steep-gradient region of the rear-side plasma.

A four-probe-pulse negative record of the rear-side expansion of a 7-micron CH foil is shown in Fig. 2A for 140J onto the target. Green probe pulses (500 psec) were used with a 2.5 nsec inter-pulse spacing, starting 2.5 nsec after the peak of the main-laser pulse. A generally smooth rear-side expansion is seen with a velocity of around 10^7 cm/sec. However, a fine-scale, filamentary-appearing structure is seen in each profile image (dark band). This can clearly be seen in the enlargement from a 430-J shot onto a 6 micron CH target shown in Fig. 2B with a 100-micron reference marker. For comparison, a bright-field shadowgram (no mask) is given in Fic. 2C. Here, the target was also a 6-micron CH foil and was irradiated with 170J. The structures seen in dark field and bright field are rather similar in shape. In bright field, the filaments are dark (appearing bright in the negative print shown) and extend into a bright background. They give the impression of being uniformly dark (as would result from absorption) and not having a light-dark structure, such as would result from diffraction or refraction. The length of the filements is consistent with time-smearing during the longer (green) probe pulses and was not seen when probing with the shorter, red pulses.

Probing with these longer pulses gives evidence (the observed fine-scale transverse structure) for fine-scale plasma inhomogeneities and gives information about the size, duration and motion of the plasma density structures. Four of the unchopped (2.5 nsec) green pulses were combined on one shot to give a very long (8 nsec) green pulse. The streaked structure for this shot could be seen to originate and terminate within the 8-nsec duration indicating a typical duration of 1 to 2 nsec. Further information about the structure was obtained from the angular distribution of the scattered green (500 psec) light. By imaging the Fourier transform plane (back-focal-plane) of L_1 it was found that the light was scattered through a half-angular range of 3 (to get past the mask) to 8 degrees. Diffraction by inhomogeneities of scale size 5 to 10 microns, as well as refraction in the region of strong density gradients, would scatter light into these angles. A limited range of scattering angles could also result from Bragg-like scattering off of a rippled or rough structure.[9,10] However, the minimum wavelength disturbance that would deflect light into the collection lens aperture ($\pm 14^{\circ}$) is 20 microns; structure smaller than this cannot be explained by this mechanism. The 8° cut-off of the observed light could not be explained by structure smaller than 60 microns, i.e. much longer than th 5 to 10 micron observed structure.

Resolution of the structure along the direction of motion requires a shorter duration probe pulse. A variety of structures have, in fact, been resolved by the Raman-shifted red pulse. Details of two types of structure can be seen in the enlargements of sections of the front shown in Fig. 3. In Fig. 3A, the target was a 4.5-micron foil of aluminum irradiated with 456 joules of laser energy. A rather narrow, smooth structure is seen. Such a structure is consistent with a stably accelerated front. A very different appearing structure is seen in Fig. 3B where a 11-micron foil target of plastic (CH) was irradiated with 480 joules. Structure in the range 5-10 microns can be seen (as suggested in earlier data by the angular scatter of green light) but there is also a vortex-like structure with dimensions around 30 microns. This structure, seen 2.5 nsec after the peak of the main pulse, could be the remnants of a hydrodynamic instability which occurred at an earlier time and higher density.

A third type of structure is seen in Fig. 4. The entire front is shown in Fig. 4A for a thin (6 micron) plastic foil irradiated by 496 joules of laser energy. The distance marker is 1 mm. An enlargement of a section of this front is shown in Fig. 4B. A definite fringe-like structure is seen. The fringe spacing (11 microns) is about right for a multiple pulse (interval of 80 psec) exposure of a sharply defined ($\sim$ 5 microns), moving (10^7 cm/sec) plasma front. However, the fringes are very regular and sharply defined and this shot had a brighter-than-average probe pulse. Also, this was a very energetic main laser shot (496J) onto a thinner than usual (6 micron) plastic target. Spectroscopic measurements[3] have shown that the rear-side temperature is somewhat higher for these thin, plastic targets. This is consistent with a rather gentle density gradient. Thus, the fringes are more likely to be the interference fringes, discussed next.

The bright-field, short-pulse shadowgrams (not shown) had background fringes over the entire field and were identified as resulting from an interference filter placed in front of the camera shutter. For the dark field data, these fringes were also seen in the regions which refracted the probe light strongly enough to get past the mask and be recorded. Such fringes can be seen on the front (left) side in Fig. 4A, where the spacing varies with position according to the local refraction. The fringe spacing is much smaller (11 microns) in the strongly refracting region of the rear-side plasma front as shown in the enlargement in Fig. 4B. These interference fringes, due to the filter, differ from those in ordinary interferometry in that both of the wavefronts correspond to the phase-disturbed region. Nevertheless, one can utilize these fringes to obtain relative phase shifts and local refraction angles. For a given location in the target plane, the phase shift due to refraction is superimposed on the locally linear phase shift due to the filter. All quantities are referred to the target plane. Thus, the rate of change of phase with respect to distance z normal to the fringes is $2\pi\left[(1/d_o) + (\theta/\lambda)\right]$, where d_o is the fringe spacing (110 microns) without refraction and θ is the angle of refraction.[11] This can also be expressed as $2\pi/d$, where d is the fringe spacing in the refracting region. Thus, the refraction angle is $\theta = \lambda(d_o - d)/d\,d_o$, or 3^o. This is light which just clears the mask and is consistent with refraction from a region of rather gentle gradients - as hypothesized earlier.

There is considerable interest in the rear-side temperature since a high pellet gain can only be achieved with a low-isentrope fuel region.[2] The dark-field (long pulse) data showed evidence that the structure is relatively cold ($\sim$1 eV). One bit of evidence is the observed lifetime of 1 to 2 nsec. For a 5-10 micron density structure to survive for this time, the sound velocity must be a few times 10^5 cm/sec, which implies a temperature around 1 eV. The other evidence is in the limited (8^o) scattering angle. This would result from the absorption in a cold plasma which prevents the probe light from reaching the region of steeper gradients which (as observed on the front side) would allow the probe light to be scattered into larger angles. These results are consistent with spectroscopic studies[3] which show that a somewhat higher density region of the rear-side plasma is relatively cold ($\lesssim$10 eV).

In summary, we have described and analyzed a dark-field, laser probing diagnostic which allows the preferential sampling of the leading (steep gradient) region of a rapidly expanding plasma and permits two-dimensional, multiple-time recordings on a single photograph. Both long and short probe pulses were used to study the rear-side plasma of a laser-accelerated foil. The longer pulse results, both for the angular scatter and the life-time of small transverse structure, implied a relatively cold (~1 eV) plasma. The short pulses provided high-resolution photographs of the complete structure. One of these was a vortex-like structure, suggestive of the remnants of a hydrodynamic instability. Refraction by the density gradients was inferred from interference fringes.

The authors wish to acknowledge useful discussions with B.H.Ripin, S.E. Bodner and R.H. Lehmberg. The technical assistance of N. Nocerino, E. Turbyfill, M. Fink, R. McGill and L. Seymour is greatly appreciated. The work was supported by the U.S. Department of Energy.

REFERENCES

1. B.H. Ripin, R. Decoste, S.P. Obenschain, S.E. Bodner, E.A. McLean, F.C. Young, R.R. Whitlock, C.M. Armstrong, J. Grun, J.A. Stamper, S.H. Gold, D.J. Nagel, R.H. Lehmberg and J.M. McMahon, Phys. Fluids 23, 1012 (1980).
2. J.L. Nuckolls, L. Wood, A. Thiessen, and G. Zimmerman, Nature (London) 239, 139 (1972).
3. E.A. McLean, S.H. Gold, J.A. Stamper, R.R. Whitlock, H.R. Griem, S.P. Obenschain, B.H. Ripin, S.E. Bodner, M.J. Herbst, S.J. Gitomer, and M.K. Matzen, Phys. Rev. Lett. 45, 1246 (1980).
4. S.E. Bodner, to be published in the Journal of Fusion Energy.
5. M. Maier, W. Kaiser, and J.A. Giordmaine, Phys. Rev. Lett. 17, 422 (1966).
6. One can use dark field illumination to record slower moving fronts by utilizing a streak camera to shift the images. See K. Rashidi and S.E. Ramsden in Proceedings of the Eleventh International Congress on High Speed Photography, Imperial College, University of London, Sept. 1974, Edited by P.J. Hall (Chapman and Hall, London 1975), p. 380.
7. J.W. Goodman, Introduction to Fourier Optics, (McGraw-Hill; New York 1968), p. 111.
8. M. Born and E. Wolf, Principles of Optics, Second Edition (Pergammon Press, New York, 1964), p. 425.
9. P. Beckman and A. Spizzichino, The Scattering of Electromagnetic Waves from Rough Surfaces, (Plenum, New York 1963), p. 34.
10. B.H. Ripin in NRL Memo Report No. 3591 (1977), pg. 128-177, unpublished; B.H. Ripin in IEEE J. Quant. Elec. QE-13, 796-34D (1977).
11. J.A. Stamper, Appl. Opt. 19, 3053 (1980).

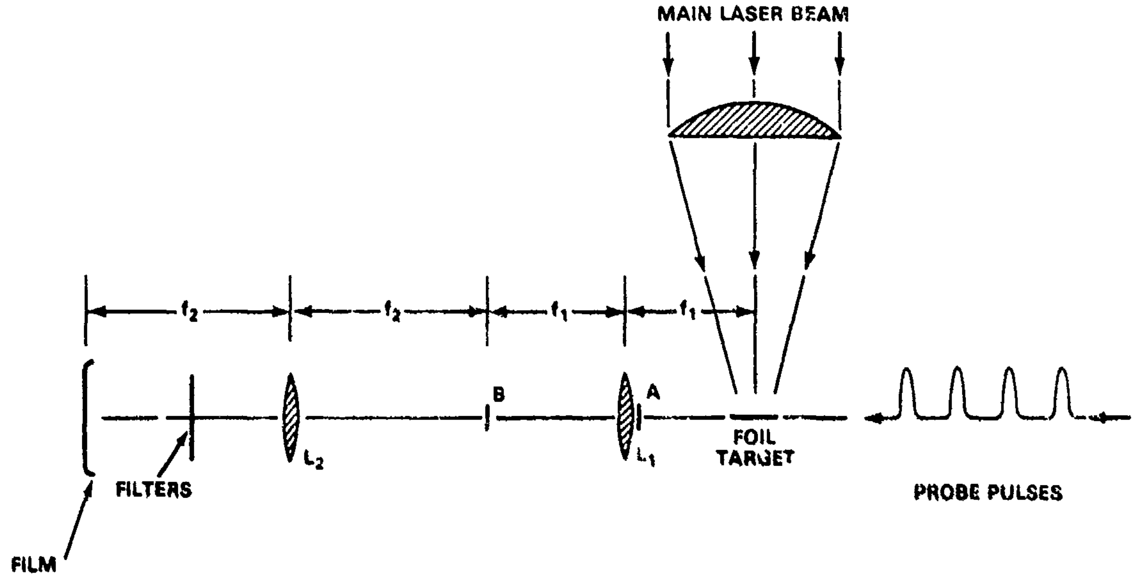

Fig. 1 — Experimental arrangement

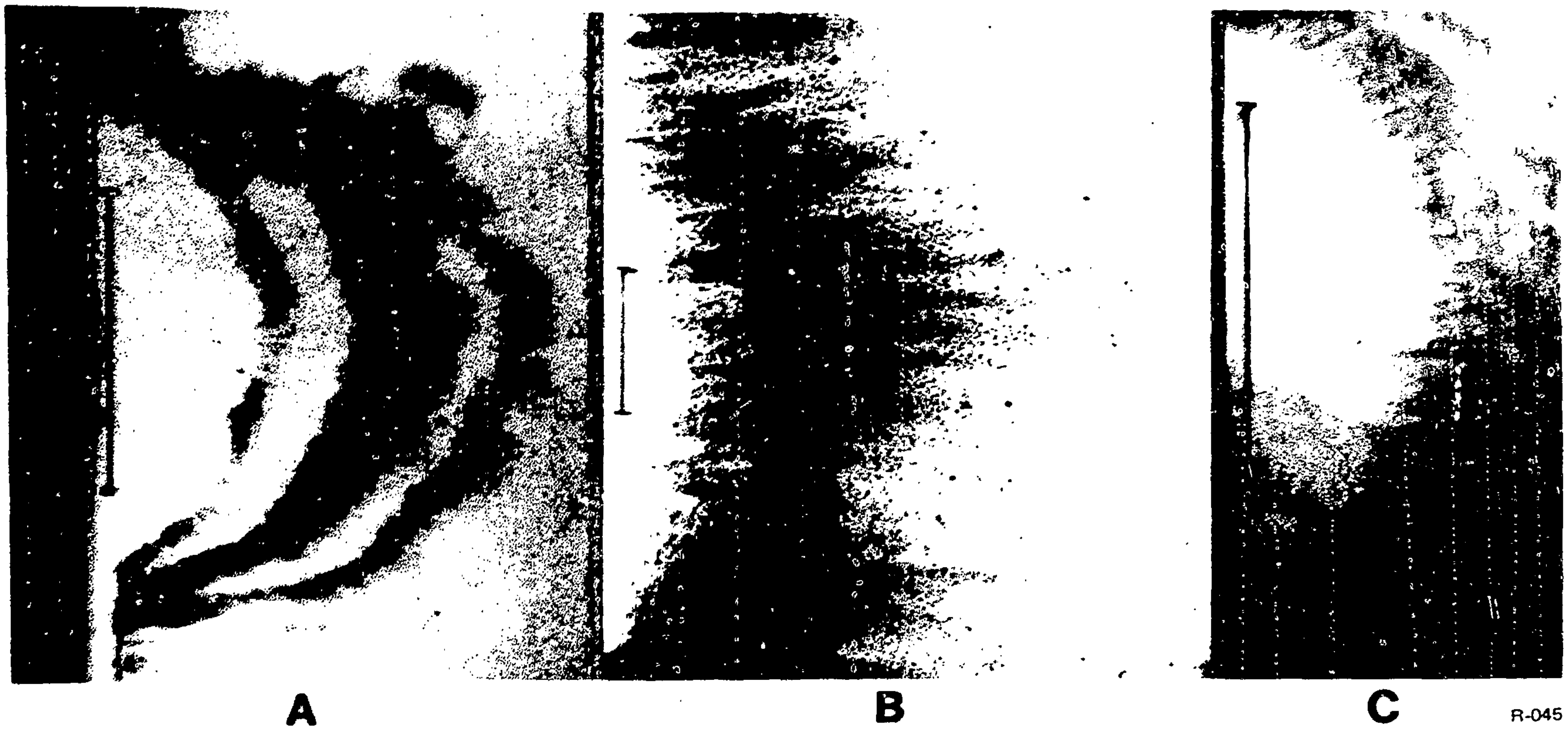

Fig. 2 – Negative photographs of rear-side plasmas for long-pulse (500 psec), green (5270 Å) probing. The laser is incident from the left. (A) Four-time, dark-field shadowgram for a 7-micron CH foil irradiated with 144J and probed at 2.5 nsec intervals starting 2.5 nsec after the peak of the main laser. Reference is 1 millimeter. (B) An enlargement of a single-time (+2.5 nsec), dark-field shadowgram for 430 J onto a 6-micron CH foil. Reference is 100 microns (C) A single-time (+4 nsec), bright-field shadowgram for 170J onto a 6-micron CH foil. Reference is 1 millimeter. These long-pulse shadowgrams show a fine-scale transverse structure and a filamentary appearance due to time-smearing.

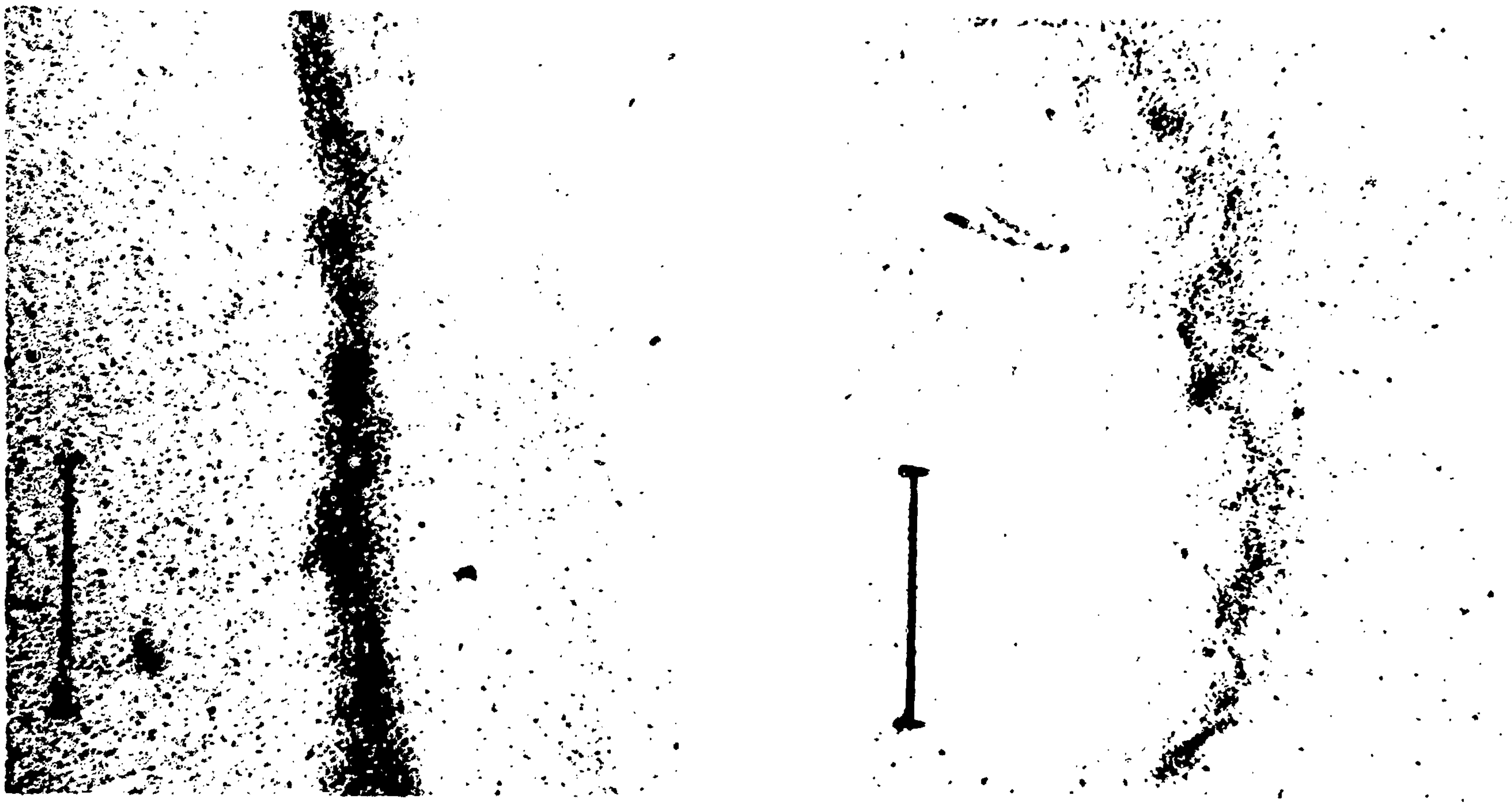

A B R-044

Fig. 3 — Single-time, dark-field photographs of enlarged sections of two rear-side structures resolved with the short (6258 Å) probe pulse. The laser is incident from the left. The reference markers are both 100 micron. A relatively smooth structure is shown in (A) for a 4.5 micron aluminum target irradiated with 456J. A vortex-like structure is shown in (B) for a 11 micron CH target irradiated with 180J

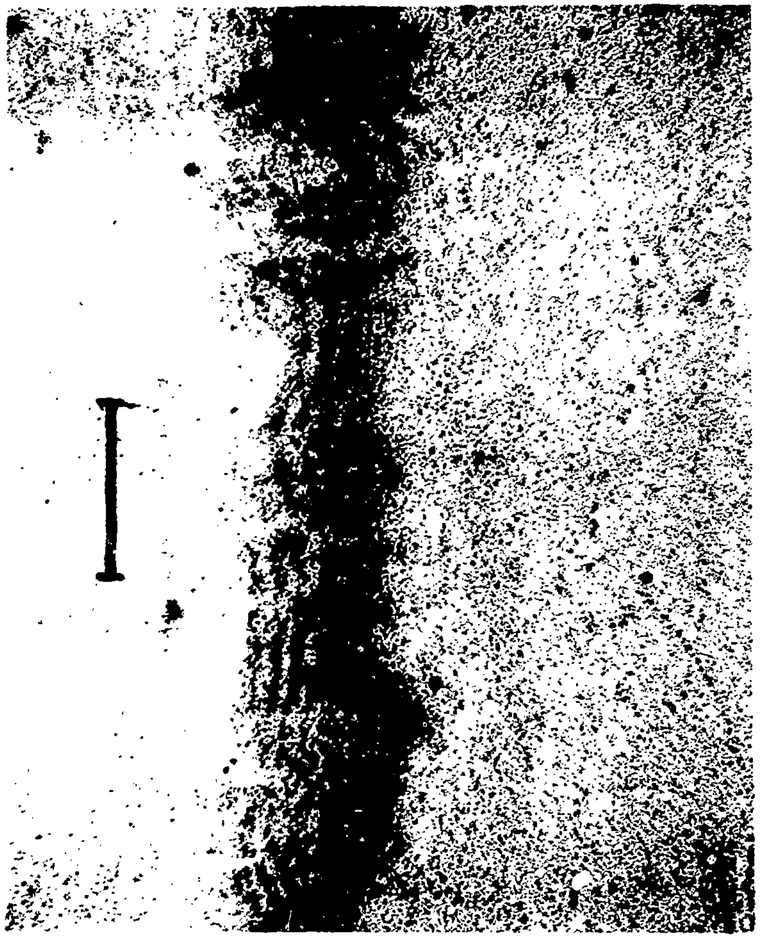

A B

R-043

Fig. 4 — Short probe, dark-field, negative photographs of a rear-side plasma front for a 6-micron CH target irradiated with 496J. The laser is incident from the left. (A) is a view of the entire profile with a 1 millimeter reference marker. Note on the front (left) side, fringes that are present in the light refracted by the front-side plasma. An enlargement of a section of the rear-side plasma is shown in (B). This shows interference fringes (discussed in the text) with a 11-micron spacing. A 100-micron reference marker is shown.

DISTRIBUTION LIST

USDOE (50 copies)
P.O. Box 62
Oak Ridge, TN 37830

National Technical Information Service (24 copies)
U.S. Department of Commerce
5285 Port Royal Road
Springfield, VA 22161

NRL, Code 2628 (35 copies)

NRL, Code 4730 (100 copies)

NRL, Code 4700 (25 copies)

USDOE (6 copies)
Office of Inertial Fusion
Washington, D.C.
Attn: Dr. G. Canavan
Dr. R. Schriever
Dr. S. Kahalas
Dr. T. Godlove
Dr. K. Gilbert

Lawrence Livermore Laboratory
P.O. Box 808
Livermore, CA 94551
Attn: Dr. D. Attwood, L481
Dr. W. Kruer, L545
Dr. J. Lindl, L32
Dr. C. Max, L545
Dr. A. Glass
Dr. L. Coleman
Dr. J. Nuckolls
Dr. W. Mead
Dr. N. Ceglio
Dr. R. Kidder

INTERNAL DISTRIBUTION

Code 4790 Dr. D. Colombant
Dr. W. Manheimer

Department of Physics and Astronomy
University of Maryland
College Park, MD 20740
Attn: Dr. H. Griem

Los Alamos Scientific Laboratory
Los Alamos, NM 87545
Attn: Dr. R. Godwin
Dr. S. Gitomer
Dr. J. Kindel

University of Rochester
Rochester, NY 14627
Laboratory for Laser Energetics
Attn: Dr. J. Soures
Dr. W. Seka

KMS Fusion
3941 Research Park Drive
P.O. Box 1567
Ann Arbor, MI 48106
Attn: Dr. F. Mayer

Institut fur Plasmaphysik
8046 Garching
Bei Munchen
West Germany
Attn: Dr. R. Sigel

National Research Council
Division of Physics
100 Susser Drive
Ottawa KIA-OR6, Canada
Attn: Dr. J. Alcock

University of Quebec
INRS Energie
Case Postale 1020
Varennes, Quebec
Attn: Dr. T. Johnston
Dr. R. Decoste

Rutherford Laboratory
Chilton, Didcot
Oxon OX110QX
England
Attn: Dr. M. Key
Dr. T. Raven

Sandia Laboratory
Albuquerque, NM
Attn: Dr. K. Matzen
Dr. J. Anthes
Dr. R. Palmer

Institute for Laser Engineering
Osaka University
Suita Osaka, 565
Japan
Attn: Dr. C. Yamanaka

Shanghai Institute of Optics and Fine Mechanics
Academia Sinica
Shanghai, PRC
Attn: Prof. Gan Fu-xi
Prof. Yu Wen-yan
Prof. Xu Zhi-zhan
Prof. Deng Xi-ming
Prof. Tan Wei-han
Mr. Pan Cheng-min

Soreq Nuclear Center
Yavne, Israel
Attn: Dr. A. Krumbein

INTERNAL DISTRIBUTION

Code 4040 J. Boris
J. Gardener
J. Orens

Dr. James Lunney
Dept. of Pure and Applied Physics
Queens University
Belfast, N. Ireland

Defense Technical Information Center
Cameron Station
5010 Duke Street
Alexandria, VA 22314